

Short communication

# A commercial-grade 1.2-V/6-Ah nickel/metal hydride cell

V. Ganesh Kumar <sup>a</sup>, K.M. Shaju <sup>a</sup>, N. Munichandraiah <sup>b</sup>, A.K. Shukla <sup>a,\*</sup>

<sup>a</sup> Solid State and Structural Chemistry Unit, Indian Institute of Science, Bangalore, 560 012, India

<sup>b</sup> Department of Inorganic and Physical Chemistry, Indian Institute of Science, Bangalore, 560 012, India

Received 8 May 1998; accepted 19 May 1998

## Abstract

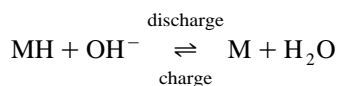
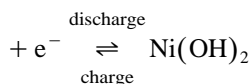
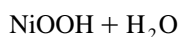
The performance of a commercial-grade 1.2-V/6-Ah nickel/metal hydride cell is reported in terms of discharge characteristics and cycle life. The cell is comprised of compacted, metal hydride negative electrodes, made out of a stoichiometric AB<sub>2</sub>-Laves phase with nominal composition Zr<sub>0.5</sub>Ti<sub>0.5</sub>V<sub>0.6</sub>Cr<sub>0.2</sub>Ni<sub>1.2</sub>, and sintered nickel positive electrodes. The cell can withstand prolonged charge–discharge schedules with little deterioration in performance. The effect of varying discharge rate and temperature is also examined. © 1998 Elsevier Science S.A. All rights reserved.

**Keywords:** Nickel metal/hydride cells; Laves phase; Hydrogen-storage alloys; Cycle life; Discharge rate

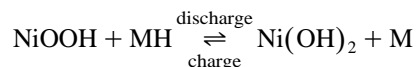
## 1. Introduction

The nickel/metal hydride cell is similar to the nickel/cadmium cell but with hydrogen absorbed in a metal alloy as the negative active material in place of cadmium. The replacement of cadmium not only increases the specific energy but also produces a more environmental friendly power source with less disposal problems [1–4]. As in the nickel/cadmium cell, the electrolyte is concentrated aqueous KOH.

The half-cell reactions during charge and discharge of the nickel/metal hydride cell are:



The overall cell reaction is:



The cell has a voltage ( $E_{\text{cell}}$ ) in the range 1.32 to 1.35 V, which is marginally higher than the voltage (1.29 V) of the nickel/cadmium cell; this makes the two cells easily interchangeable. In addition, there is no net change in either the quantity or the concentration of the electrolyte with charge–discharge cycling. This contrasts with the nickel/cadmium cell, where water is generated during charge and consumed during discharge [3,4]. For the successful operation of a nickel/metal hydride cell, however, it is essential to employ an appropriate hydrogen-storage alloy as the negative-electrode material. The various alloys that have been employed as negative-electrode materials in nickel/metal hydride cells belong to the AB<sub>2</sub> and the AB<sub>5</sub> series; partial substitution of one or other of the two components in the alloy is imperative to provide an optimized negative electrode [5–7]. After a systematic screening of various AB<sub>2</sub> and AB<sub>5</sub> alloys, we have found that negative electrodes with an AB<sub>2</sub> alloy of composition Zr<sub>0.5</sub>Ti<sub>0.5</sub>V<sub>0.6</sub>Cr<sub>0.2</sub>Ni<sub>1.2</sub> can yield a discharge capacity value of about 300 mAh g<sup>-1</sup>, sufficient to suggest that the cell construction has practical merit.

In this communication, we report a commercial size, 1.2-V/6-Ah nickel/metal hydride cell with a positive-limited configuration. The effect of varying discharge rate

\* Corresponding author. Tel.: +91-80-309-27 95; Fax: +91-80-331-13-10; E-mail: shukla@sscu.iisc.ernet.in

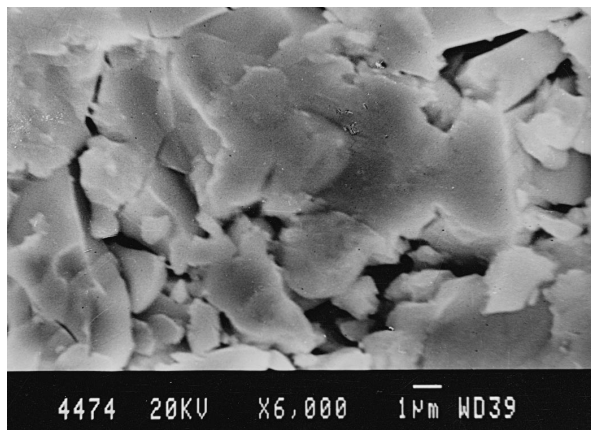


Fig. 1. Electron micrograph of alloy.

and operational temperature on the performance of the cell have been studied. Cycle-life tests suggest that the rated capacity can be delivered over prolonged charge/discharge schedules.

## 2. Experimental details and results

### 2.1. Preparation and characterization of negative-electrode material

An ingot of  $Zr_{0.5}Ti_{0.5}V_{0.6}Cr_{0.2}Ni_{1.2}$  alloy that weighed about 600 g was obtained by arc melting the spongy constituent elements under argon atmosphere at  $10^{-3}$  to  $10^{-4}$  Pa in a water-cooled copper crucible. Morphological and compositional analyses of the alloy were carried out on a JEOL-JSM-840A Scanning Electron Microscope linked to an Oxford-ISIS Elemental Analyzer. An electron micrograph of the alloy is shown in Fig. 1. Its elemental

Table 1  
Elemental composition of alloy sample as obtained from EDAX

Element	Spectral line	Element %	Atomic %	Stoichiometry
Zr	L-ED	24.75	16.33	0.49
Ti	K-ED	12.18	15.33	0.46
V	K-ED	18.33	21.67	0.65
Cr	K-ED	6.05	7.00	0.21
Ni	K-ED	38.69	39.67	1.19
Total		100.00	100.00	3.00

composition, as obtained from energy dispersive analysis of X-rays (EDAX) by averaging the results from ten randomly chosen spots, is found to be  $Zr_{0.49}Ti_{0.46}V_{0.65}Cr_{0.21}Ni_{1.19}$  (see Table 1) which is in good agreement with the composition determined from quantitative chemical analysis of the constituent elements. This phase is stoichiometrically different from that reported by Miyamura et al. [8]. The powder X-ray diffraction (XRD) pattern of the alloy sample, obtained by means of a JEOL-JDX-8P diffractometer using  $CuK\alpha$  radiation, is shown in Fig. 2. The XRD pattern is typical of a hexagonal  $AB_2$  alloy. Using these data, the lattice parameters of the alloy are found to be:  $a = 4.97 \text{ \AA}$  and  $c = 8.11 \text{ \AA}$ . The alloy was mechanically crushed and sieved to obtain alloy particles in the size range 49 to 73  $\mu\text{m}$ . The hydrogen absorption and desorption characteristics of the alloy were determined by obtaining the pressure–composition isotherm with a Sieverts' apparatus. The isotherm is given in Fig. 3 and suggests that the alloy can facilitate absorption/desorption of hydrogen at ambient conditions.

### 2.2. Fabrication and formation of negative electrodes

Roll-compacted negative electrodes were prepared from the dough obtained by mixing alloy (85 wt.%), graphite powder (10 wt.%), and polytetrafluoroethylene (PTFE)-

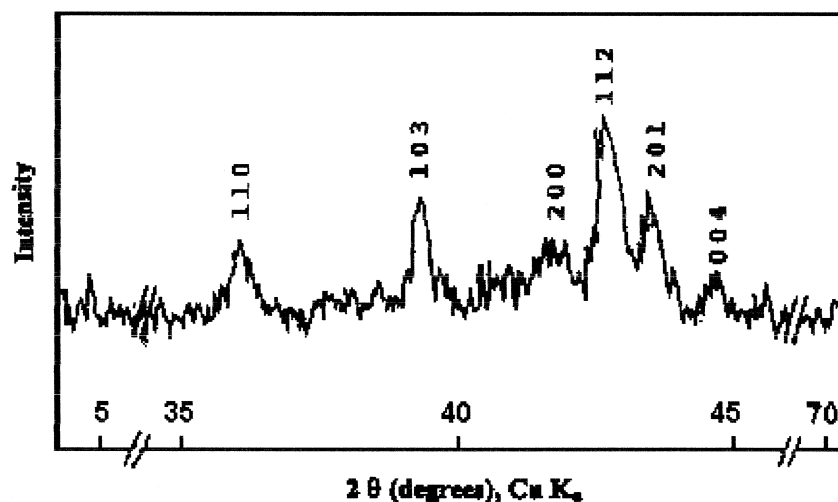


Fig. 2. Powder X-ray diffraction pattern of alloy.

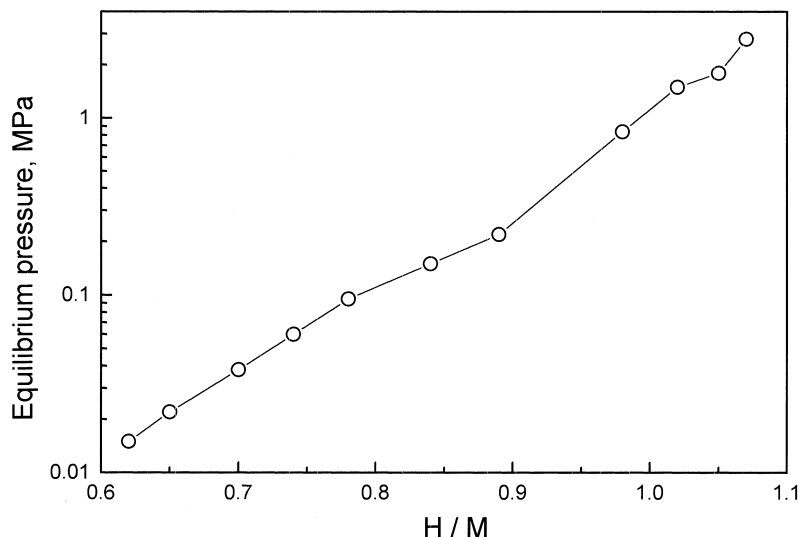


Fig. 3. Pressure–composition isotherm of alloy at 30°C.

GP2 Fluon suspension (5 wt.%) in an ultrasonic agitator. The resulting putty-like mass was rolled against a smooth steel plate. The rolled sheet of the active material with additives was folded around a degreased nickel mesh (dimensions:  $56 \times 50 \times 0.1$  mm) and pressed at an optimum compaction pressure of  $3000 \text{ kg cm}^{-2}$  for 15 min. The roll-compacted electrodes were heat-treated in a gas stream which comprised 10% hydrogen and 90% argon at

623 K for 30 min. The physical thickness of the finished electrodes was about 1 mm.

The metal–hydride electrodes thus prepared were subjected to formation in electrochemical cells which contained 6 M KOH electrolyte. Sintered nickel hydroxide electrodes were placed on either side of the metal–hydride electrode in each of the cells. The metal–hydride electrodes were found to form and achieve their rated capacity values within about 5 charge–discharge cycles. During the first cycle, the electrodes were charged at the C/20 rate and, subsequently, at the C/10 rate. The electrodes are typically discharged at the C/5 rate. The metal–hydride electrodes were inserted into pockets made out of polypropylene separator cloth.

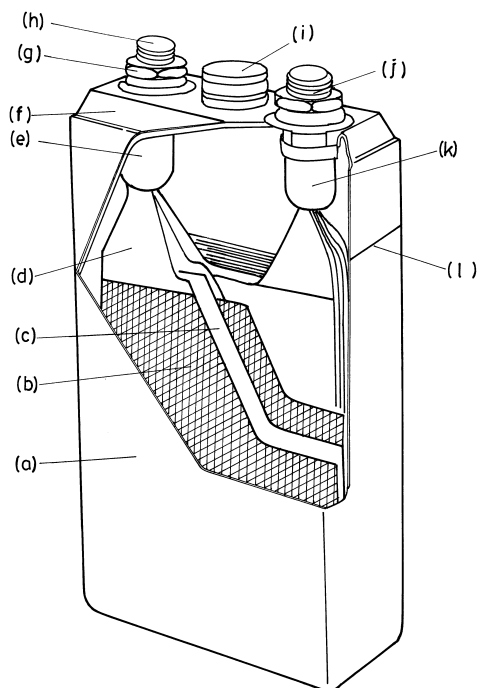


Fig. 4. Schematic diagram of 1.2-V/6-Ah nickel/metal hydride cell: (a) container; (b) negative plate wrapped with separator cloth; (c) positive plate; (d) plate frame; (e) negative lug; (f) cell lid; (g) locking nut; (h) negative terminal; (i) vent; (j) positive terminal; (k) positive lug; (l) electrolyte level.

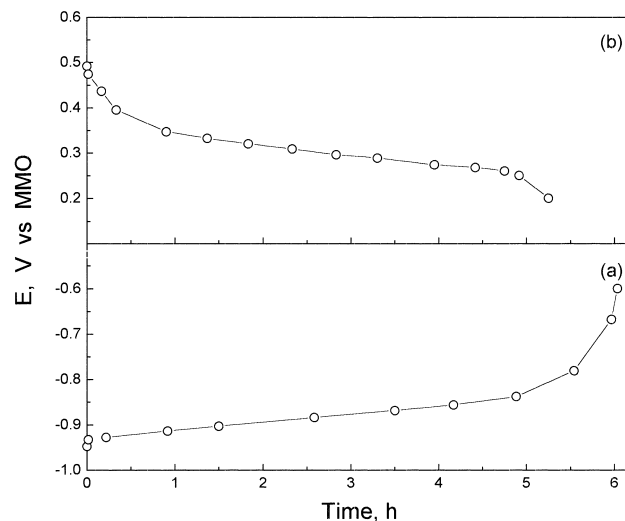


Fig. 5. Typical discharge data obtained at a C/5 rate and 30°C for: (a) metal–hydride negative; (b) nickel–positive electrodes employed in the nickel/metal hydride cell assembly.

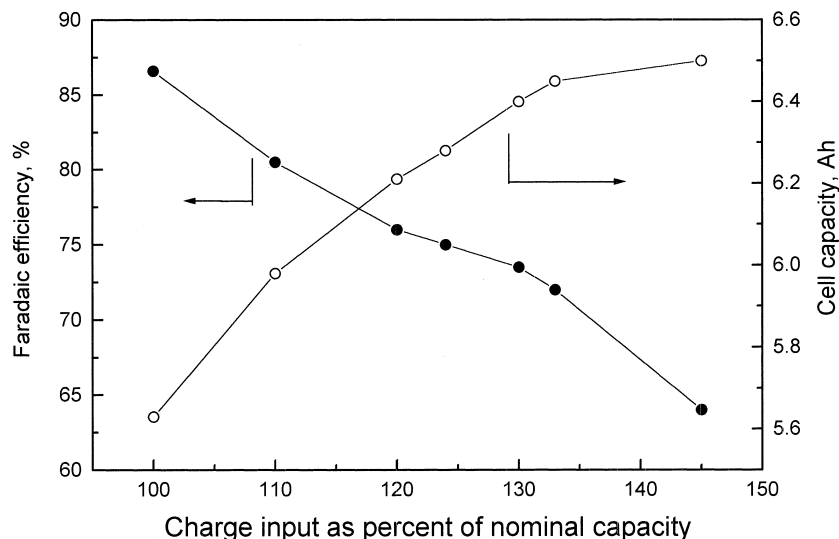


Fig. 6. Capacity and Faradaic efficiency data for nickel/metal hydride cell at 30°C and various charge inputs.

### 2.3. Cell assembly

Positive-limited, nickel/metal hydride secondary cells were assembled by alternatively stacking nine commercial-grade nickel-positive electrodes (average capacity: 0.8 Ah) and ten metal-hydride negative electrodes (average capacity: 0.8 Ah). The positive and negative electrodes were welded to the respective lugs and then placed in a poly-propylene container (dimensions: 90 × 57 × 33 mm) which could withstand the concentrated alkali environment without deterioration for long durations and

temperatures up to about 45°C. The cells were filled with 6 M KOH electrolyte so as to soak the electrodes completely. A schematic diagram of such a cell is shown in Fig. 4.

### 2.4. Performance characteristics of nickel / metal hydride cells

Typical data for the discharge characteristics of the metal hydride-negative and nickel-positive electrodes, employed for an assembly of 1.2-V/6-Ah nickel-metal hy-

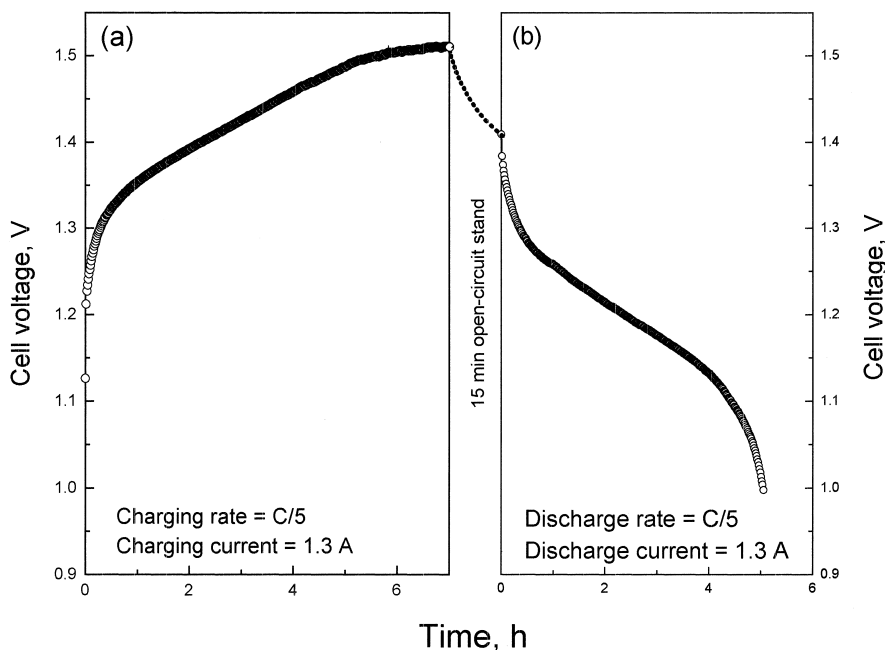


Fig. 7. Typical (a) charge, and (b) discharge data for nickel-metal hydride cell at the C/5 rate and 30°C.

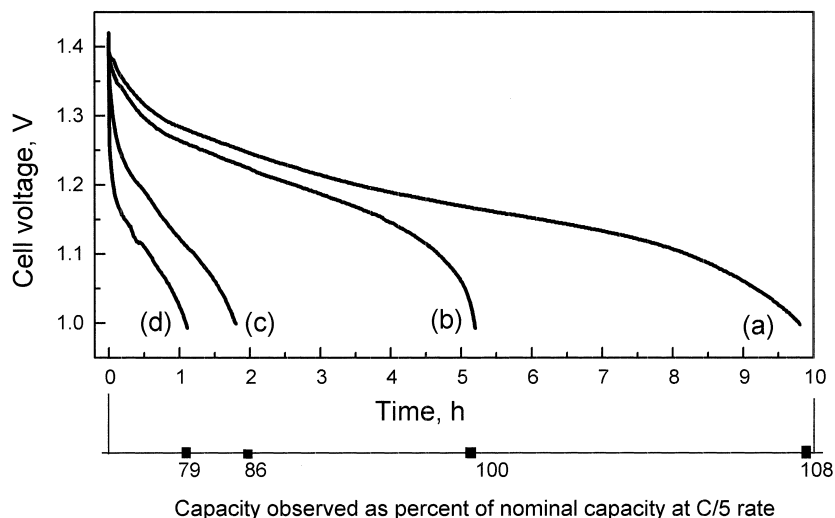


Fig. 8. Performance of nickel/metal hydride cell at 30°C and various discharge rates, viz., (a) C/10, (b) C/5, (c) C/2, (d) C.

hydride cells are shown in Fig. 5. The metal-hydride electrodes were discharged up to  $-0.6$  V versus Hg/HgO,  $\text{OH}^-$  (MMO) reference electrode. On an average, the electrodes delivered a capacity of 800 mAh ( $\sim 300 \text{ mAh g}^{-1}$ ) at the C/5 rate (corresponding current = 150 mA). The nickel-positive electrodes were found to yield an average capacity of 800 mAh at the C/5 rate. The capacity of the nickel electrodes showed little variation in capacity at discharge rates between C and C/5.

The Faradaic efficiency of the cell at 30°C at a C/5 charge-discharge rate is shown in Fig. 6. The data show a maximum Faradaic efficiency for the cell at 100% charge input with a cell capacity as low as 5.6 Ah. At 135% charge input, the cell was found to deliver a capacity value of 6.5 Ah. Accordingly, other experiments on the cells were performed after giving 135% charge at C/5 rate.

Typical charge-discharge data for the cell at the C/5 rate are shown in Fig. 7. The cell exhibits an initial drop of 50 mV and thus indicates that its internal resistance is about  $40 \text{ m}\Omega$ . At the C/5 rate, the cell has been found to deliver a nominal capacity of 6.5 Ah up to a cut-off voltage of 1 V. The performance of the cell at various discharge rates is presented in Fig. 8. The cell shows a loss of nearly 20% in its nominal capacity as its discharge rate is varied from C/5 to C at 30°C.

The effect of temperature on the discharge characteristics of the cell at the C/5 rate is shown in Fig. 9. The cell suffers a loss of nearly 20% of its nominal capacity as its temperature is raised from 30 to 40°C. Interestingly, the cell shows an increase of about 10% in its nominal capacity at 20°C. The cell was subjected to a charge stand for 115 h at 30°C and retained about 80% of its nominal

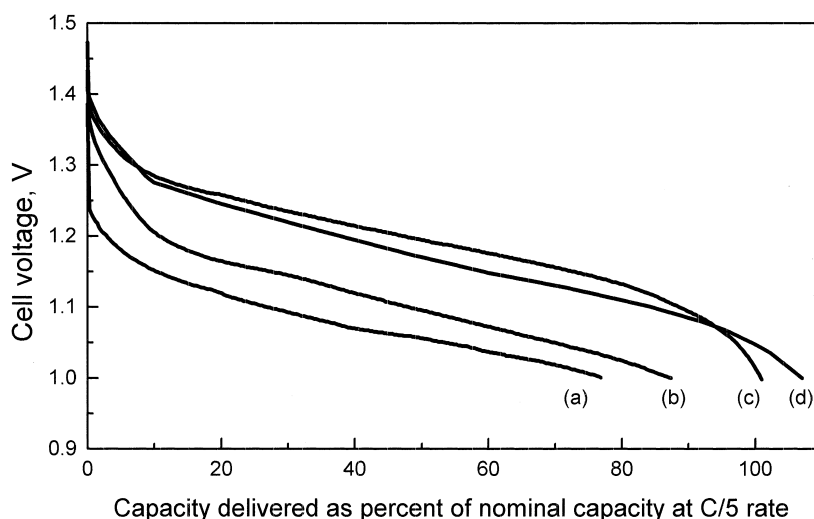


Fig. 9. Capacity of nickel/metal hydride cell at various temperatures at C/5 rate: (a) 40°C, (b) 5°C, (c) 30°C, and (d) 20°C.

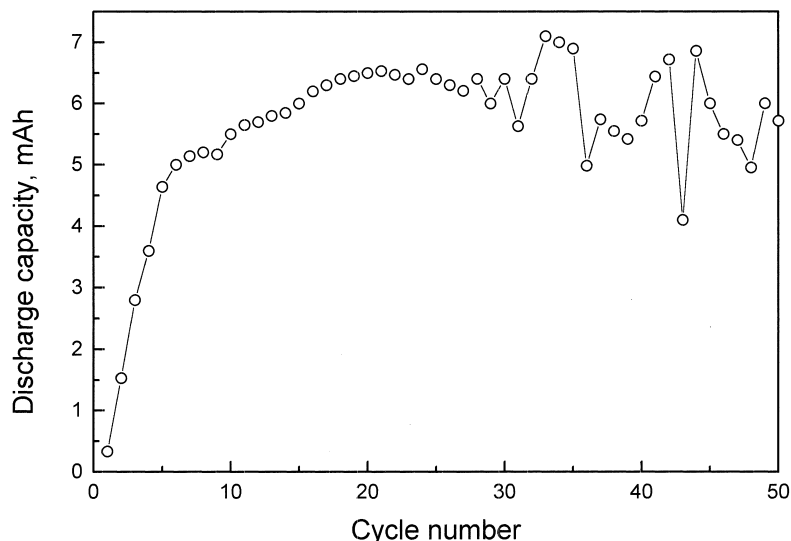


Fig. 10. Cycle-life of nickel/metal hydride cell.

capacity. This suggests that the self-discharge rate is about 4% per day. The rate of self-discharge of the cell is, however, dependent on both the storage temperature and time. The longer the storage time, the lower the rate of self-discharge for the cell. It is found that the rate of self-discharge of the cells was only 2% per day over the storage time of 30 days. At 20°C and below, the self-discharge of the cell is considerably less, viz., 0.1 to 1% of the nominal capacity per day on the average, depending on the temperature. The cycle-life data for the cell are given in Fig. 10. The positive-limited configuration of the cell facilitates oxygen recombination, as reflected by a small  $-\Delta V$  effect during overcharge of the cells. The cells have completed about 50 charge–discharge cycles at the C/5 rate without any noticeable loss in their nominal capacity. The fluctuations seen in the capacity values of the cell beyond 30 cycles are due to variations in temperature and rate of discharge.

### 3. Conclusion

The study suggests that the  $AB_2$ -alloy system with nominal composition  $Zr_{0.5}Ti_{0.5}V_{0.6}Cr_{0.2}Ni_{1.2}$  can be successfully employed for producing commercial-grade

nickel–metal hydride cells with optimum performance at 20°C.

### Acknowledgements

We thank DMRL-Hyderabad and M/S Renewable Energy Systems-Hyderabad for their help. Financial support from Indian Space Research Organisation is gratefully acknowledged.

### References

- [1] D. Linden, in: D. Linden (Ed.), Handbook of Batteries, McGraw Hill, New York, 1995, pp. 33.1–33.29.
- [2] S.R. Ovshinsky, M.A. Fetcenko, J. Ross, Science 260 (1993) 176.
- [3] N. Furukawa, J. Power Sources 51 (1994) 45.
- [4] M.A. Fetcenko, S. Venkatesan, S.R. Ovshinsky, in: D.A. Corrigan, S. Srinivasan (Eds.), Proc. Electrochemical Soc., Vol. 92-5, The Electrochemical Society, Pennington, NJ, 1992.
- [5] D.G. Westlake, J. Less-Common Metals 91 (1983) 1.
- [6] A. Anani, A. Visintin, K. Petrov, S. Srinivasan, J.J. Reilly, J.R. Johnson, R.B. Schwarz, P.B. Desch, J. Power Sources 47 (1994) 261.
- [7] S.K. Dhar, S.R. Ovshinsky, P.R. Gifford, D.A. Corrigan, M.A. Fetcenko, S. Venkatesan, J. Power Sources 65 (1997) 1.
- [8] H. Miyamura, T. Sakai, N. Kuriyoma, K. Oguro, I. Uehara, H. Ishikawa, Z. Physik. Chem. NF 183 (1994) 347.